

Cite this: *J. Mater. Chem. C*, 2017, 5, 4716

Adamantane substitutions: a path to high-performing, soluble, versatile and sustainable organic semiconducting materials†

Alexander Kovalenko,^a Cigdem Yumusak,^b Patricie Heinrichova,^a Stanislav Stritesky,^a Ladislav Fekete,^c Martin Vala,^a Martin Weiter,^a Niyazi Serdar Sariciftci^b and Jozef Krajcovic^a

Novel ethyladamantyl solubilization side groups were found to induce π - π interactions between the conjugated cores through adamantyl-adamantyl stacking in soluble diketopyrrolopyrrole (DPP) derivatives. The closeness of the DPP cores amplifies charge transfer in the material, as far as the π - π interaction is a dominant charge-hopping pathway. As a result, tenfold enhancement of hole mobilities exceeding those obtained for insoluble derivatives was reached. Moreover, due to high crystallinity and co-planarity of the conjugated cores, electron transfer was preserved with a mobility of $0.2 \text{ cm}^2 \text{ V}^{-1} \text{ s}^{-1}$ for dithiophene-DPP. At the same time, the material remained soluble, which is a significant advantage for purification and processing. This approach can be universally applied for many types of semiconducting organic materials containing the imide motif, where solubilization is achieved by side-group substitution.

Received 22nd November 2016,
Accepted 13th April 2017

DOI: 10.1039/c6tc05076j

rsc.li/materials-c

1. Introduction

Soluble organic semiconducting materials have particular application potential for easily processed low-cost sustainable electronic devices. The solubility of organic π -conjugated small-molecule derivatives, such as diketopyrrolopyrroles (DPP),¹⁻⁶ epindolidiones,⁷ indigos,⁸ squaraines⁹ and many others, is usually achieved by a side-chain alkyl substitution, which is meant to interrupt inter- and intramolecular H-bonds. However, because of these bonds, soluble organic semiconducting materials are usually less stable;¹⁰⁻¹² moreover, because of the tight aggregation of π -conjugated cores through intermolecular H-bonds, insoluble materials have shown high charge-carrier mobilities for both electrons and holes.^{10,13,14} On the other hand, insolubility brings its obverse case: such materials are difficult to purify and they cannot be deposited by coating or printing techniques, which are promising ways towards the cheap mass production of organic electronics devices.¹⁵ A large diversity of organic semiconducting materials' applications is spread

throughout many fields – devices for energy storage and conversion, such as photovoltaic cells,¹⁶⁻¹⁸ batteries,¹⁹ light-emitting diodes,^{20,21} inverters,²² photoelectrochemical cells,²³ field-effect organic transistors,^{24,25} devices for medical applications, such as artificial retina²⁶ or biosensors²⁷ – which are only part of the possible applications of organic semiconductors.

In this paper, we offer a strategy to synthesize thermally stable and soluble high-performing DPP-based organic semiconductors for a wide range of electronics applications. The crucial component of the present approach is using adamantyl substitutions in solubilizing side groups. Because of its specific rigid, but strain-free structure, adamantane forms a face-centred cubic lattice, which is unusual for organic compounds.²⁸ Namely, molecules perfectly fit each other forming a rigid and stable crystal. The effect of this unusual structure on the physical properties is outstanding: the relatively small adamantane molecule has one of the highest melting points of all known hydrocarbons. This ability to self-organize into crystals with an unusually high melting point²⁹ was used to reinforce packing of π -conjugated dyes in the solid state. The above-mentioned side chain can improve solid-state fluorescence quantum yields of the materials²⁹ and significantly increase the melting point. Considering the electrical properties, a soluble DPP derivative with ethyladamantyl solubilization side groups showed an ambipolar behaviour with both hole and electron mobilities higher than the insoluble analogue. It was confirmed by X-ray diffraction (XRD) analysis that the distance between π -conjugated cores is shorter than the distance for insoluble material due to

^a Brno University of Technology, Faculty of Chemistry, Materials Research Centre, Purkyňova 118, 612 00 Brno, Czech Republic. E-mail: kovalenko.alx@gmail.com

^b Linz Institute for Organic Solar Cells (LIOS), Physical Chemistry, Johannes Kepler University Linz, Altenbergerstraße 69, 4040 Linz, Austria

^c Institute of Physics, Academy of Sciences Czech Republic v.v.i, Na Slovance 2, CZ-182 21, Prague 8, Czech Republic

† Electronic supplementary information (ESI) available. CCDC 1542005. For ESI and crystallographic data in CIF or other electronic format see DOI: 10.1039/c6tc05076j

adamantyl–adamantyl aggregations, which resulted in high charge-carrier mobilities.

2. Experimental section

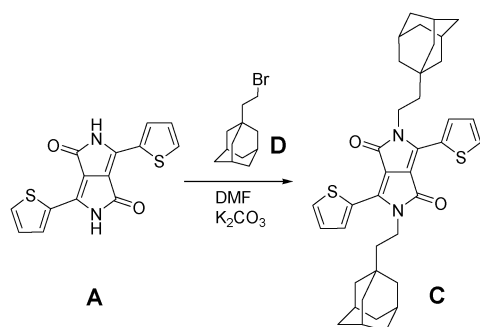
Materials

2,5-Dihydro-3,6-di-2-thienylpyrrolo[3,4-*c*]pyrrole-1,4-dione (97%), potassium carbonate (>99%, anhydrous) and *N,N*-dimethylformamide (DMF) (99.8%, anhydrous) were purchased from Sigma-Aldrich. Hexane and toluene were of analytical grade and purchased from Riedel–de Haën and used without further purification. 1-(2-Bromoethyl)adamantane (98%) was purchased from Provisco CS Ltd. Chromatographic separation was carried out on silica gel 60 (230–400 mesh, Sigma-Aldrich).

Synthesis

Anhydrous potassium carbonate (3.7 g, 26.6 mmol) was added under an Ar atmosphere to a solution of 2,5-dihydro-3,6-di-2-thienylpyrrolo[3,4-*c*]pyrrole-1,4-dione **A** (2 g, 6.6 mmol) in dry DMF (30 mL) and the mixture was heated at 90 °C for 100 min. Then, 1-(2-bromoethyl)adamantane **D** (6.5 g, 26.6 mmol) was added and the mixture was stirred for 10 h at the same temperature (Scheme 1). The suspension was filtered and the solvent was removed under reduced pressure. The crude product was purified by column chromatography on silica gel (hexane/toluene). Then, the isolated product was crystallized from toluene to afford the title product **C** as a dark violet solid (1.6 g, 38%). Melting point 323–324 °C, ¹H NMR (500 MHz, CDCl₃, δ): 8.91 (d, *J* = 3.8 Hz, 2H), 7.64 (d, *J* = 4.9 Hz, 2H), 7.27 (dd, *J* = 6, 5 Hz, 2H), 4.14–4.11 (m, 4H), 1.99–1.82 (m, 6H), 1.75–1.72 (m, 7H), 1.68–1.65 (m, 19H), 1.53–1.51 (m, 3H), ¹³C NMR (125 MHz, CDCl₃, δ): 161.27, 140.14, 135.22, 130.57, 129.69, 128.57, 107.85, 43.23, 42.30, 37.71, 37.10, 32.21, 28.63, EI [*m/z*] 624.89, found 624.97, anal. calcd for C₃₈H₄₄N₂O₂S₂: C, 73.04%, H, 7.10%, N, 4.48%, S, 10.26%. Found: C, 73.15%, H, 7.08%, N, 4.42%, S, 10.38%.

NMR spectroscopy. 500 (125) MHz ¹H (¹³C) NMR spectra were recorded on a Bruker Avance 500 spectrometer in CDCl₃. Chemical shifts (δ) are given in parts per million (ppm) relative to TMS as an internal standard. The melting point was determined on a Kofler apparatus and the temperature was not corrected. Elemental analysis was measured using an elemental analyser Flash 2000 CHNS Thermo Fisher Scientific. Mass spectra



Scheme 1 Procedure for the synthesis of the *N*-alkylated DPP derivative.

were recorded on a GC-MS spectrometer Thermo Fisher Scientific ITQ 700 (DEP).

Vacuum-deposited organic field-effect transistor (OFET) fabrication. Glass slides used for the device fabrication were cleaned sequentially with acetone, isopropanol, detergent and deionized water, and treated with O₂ plasma. 100 nm of aluminium gate electrodes were evaporated through a shadow mask. 32 nm of anodized alumina (AlO_x) was grown using the potentiostatic method.^{30,31} The AlO_x layer was then passivated by evaporating oligoethylene TTC (C₄₄H₉₀, tetratetracontane) to create an inorganic/organic composite gate dielectric with a capacitance of 20 nF cm⁻².³² 60 nm films of the DPP derivatives were evaporated at a pressure of 1 × 10⁻⁶ mbar at a rate of 0.2–0.3 Å s⁻¹. Finally, gold source and drain electrodes were evaporated using a shadow mask with a thickness of 80 nm (*L* = 60 μm, *W* = 2 mm). For the dielectric capacitance, values from the related literature^{10,32,33} were used.

Solution-processed OFET fabrication. Devices were fabricated in a bottom-gate, bottom-contact geometry on heavily doped Si wafers (Fraunhofer IPMS), consisting of a 90 nm SiO₂ layer integrated with 30 nm thick Au electrodes on a 10 nm ITO adhesion layer. The interdigital electrodes had different channel lengths (*L* = 2.5, 5, 10 and 20 μm) with a width of 1 cm. Substrates were cleaned in an ultrasonic bath of acetone and isopropyl alcohol (IPA) for 10 min and then subsequently dried with N₂. The octadecyltrichlorosilane (OTS) self-assembled monolayers (SAMs)³⁴ were formed by immersing the silicon wafers in a 10 mM toluene solution (anhydrous) for 10 min at 70 °C. Then, the substrates were rinsed with IPA and dried with N₂. Thin layers were prepared in a nitrogen glovebox. DPP layers were deposited by spin coating 15 mg mL⁻¹ of solution at 1500 rpm.

Ultraviolet-visible absorption spectroscopy. To measure the optical characteristics of each compound, thin films were deposited on quartz glass substrates by means of thermal evaporation under vacuum. The thickness of the layers was 100 ± 10 nm according to measurements on a Dektak XT mechanical profilometer (Bruker). Absorption spectra of the samples were measured using a Varian Cary Probe 50 UV-vis-near IR spectrometer, and the fluorescence spectra were obtained using a Fluorolog fluorimeter (Horiba Jobin Yvon). All optical characteristics were measured under ambient conditions.

X-ray diffraction. XRD data were collected at 120 K by the ω-scan technique on a Rigaku Saturn724 + CCD diffractometer equipped with an Oxford Cryosystem low-temperature device, using a rotating anode with MoKα radiation. The diffraction intensities were corrected for Lorentz and polarization effects and an analytical method of absorption was used. Data interpretation including all corrections mentioned previously was performed by CrystalClear-SM Expert 2.1 b32 software (Rigaku, 2014). The structures were resolved in a straightforward manner using direct methods and refined using the full-matrix least-squares method for all F₂ data. Non-hydrogen atoms were refined anisotropically, while hydrogen atoms were inserted in the calculated positions and refined isotropically assuming a ‘ride-on’ model. The SHELXS and SHELXL programs used for calculations and the XP program used for geometrical analysis were parts of the Bruker SHELXTL V5.1 program package.

Theoretical modelling (Gaussian 09). For geometry optimization, the 6-311+G** split-valence polarized triple- ζ basis set was used. As a computational method, the hybrid Becke's three-parameter functional with the Lee, Yang and Parr correlation functional (B3LYP) was applied.

3. Results and discussion

2,5-Dihydro-3,6-di-2-thienylpyrrolo[3,4-*c*]pyrrole-1,4-dione (DPP(Th)₂) (Fig. 1A), initially insoluble in organic solvents, was *N*-substituted with two types of side groups. First, the 2-ethylhexyl side chain (Fig. 1B), which has shown superior performance in both bulk-heterojunction solar cells^{35–38} and OFETs.^{3,39} Various materials including DPPs³ containing 2-ethylhexyl side chains have shown high electron³ and hole⁴⁰ mobilities, which are related to a high crystalline organization in the solid state.³⁹ Second, DPP(Th)₂ was *N*-substituted with ethyladamantyl side groups (Fig. 1C). Adamantyl-containing solubilization side groups induce high intermolecular organization in the solid, through adamantyl–adamantyl interactions,^{29,41} thus thermal stability and crystallinity can be significantly improved.

Atomic force microscopy (AFM) has shown (see Fig. 2) that all three materials are distinct from each other. The hydrogen-substituted insoluble derivative has a smooth fine-crystalline surface, whereas the soluble 2-ethylhexyl-substituted sample had separate inclusions of larger crystallites. The ethyladamantyl

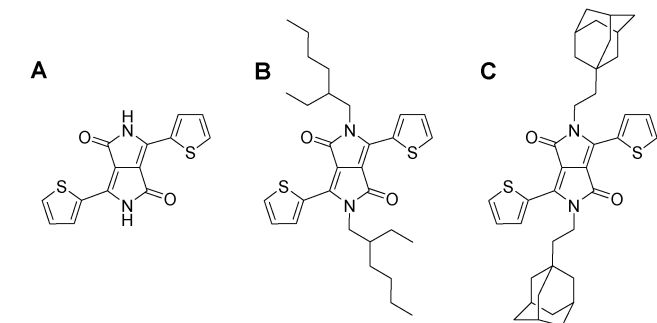
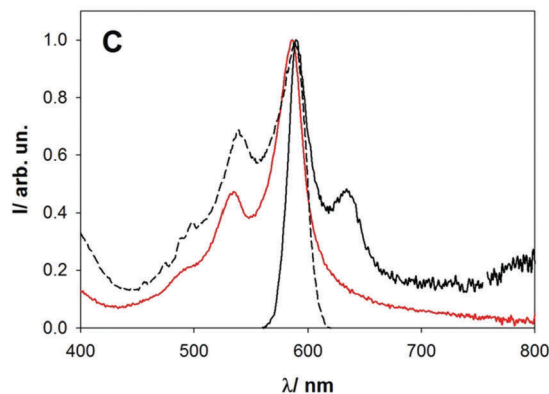
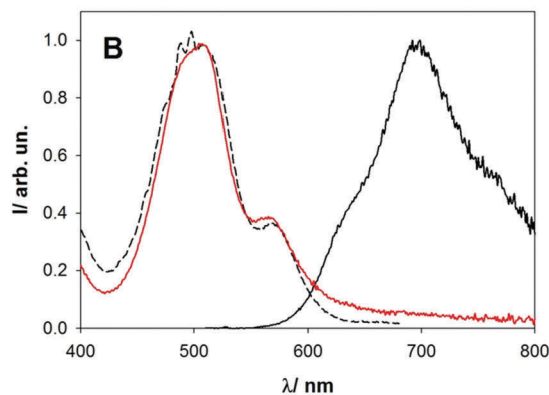
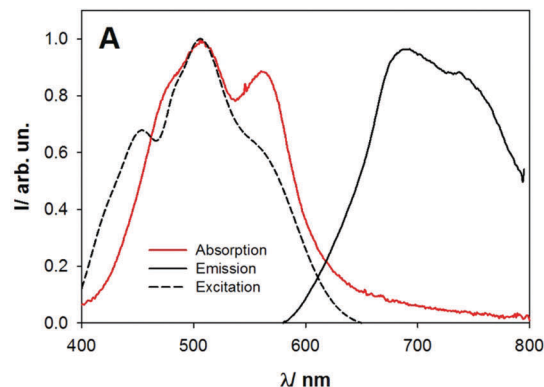


Fig. 1 Molecular structures of (A) H; (B) 2-ethylhexyl and (C) ethyladamantyl *N*-substituted DPP(Th)₂.

Fig. 3 Absorption and emission spectra of the thin films: hydrogen (A), 2-ethylhexyl (B) and ethyladamantyl (C) *N*-substituted DPP derivatives.

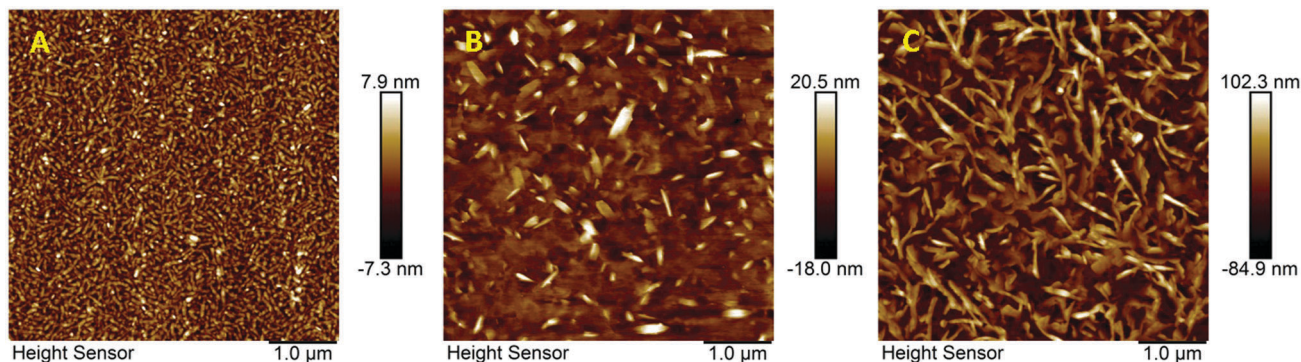


Fig. 2 AFM images of hydrogen (A), 2-ethylhexyl (B) and ethyladamantyl (C) *N*-substituted DPP derivatives.

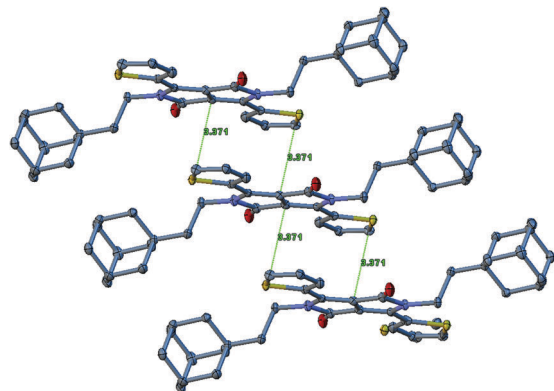


Fig. 4 Plane-to-plane stacking of ethyladamantyl-substituted DPP (XRD measurements).

N-substituted sample had a well-defined structure with large branch-like crystallites.

3.1. Optical properties

Side-chain engineering^{42,43} is a common way to alter the optical and electrical properties of organic conjugated materials, especially polymers and small molecules containing the imide motif. DPP is known to be a versatile dye, and several approaches have reported that improved properties can be reached by side-chain engineering.^{44,45} Regarding the optical spectra, side-chain engineering of DPP derivatives usually does not result in any significant changes if alkyl-derived chains are used because of the absence of side-group/core conjugation. However, it was noted that, distinctively from other compounds, the ethyladamantyl-substituted derivative (C) exhibited solid-state blue-shifted fluorescence in comparison with 2-ethylhexyl- and hydrogen-substituted derivatives. Optical spectra, depicted in Fig. 2, show that material (C) has a small Stokes shift. A negligible Stokes shift alongside well-defined vibrational peaks on the spectra is also evidence of the high crystallinity of the layer (Fig. 3).

3.2. X-Ray diffraction

To study the solid-state packing and molecular interactions of compound (C), single crystals were grown from dichloromethane:methanol (8:2 v/v) solution by slow evaporation of the solvents at room temperature. XRD parameters of the 2-ethylhexyl *N*-substituted compound (B) were taken from the previously reported paper by Naik *et al.*⁴⁶

Interestingly, according to the XRD measurements (CCDC number: 1542005), the distance between conjugated DPP cores in the case of plane-to-plane aggregations is only 3.37 Å (Fig. 4). For comparison, previously reported hexyl- and 2-ethylhexyl *N*-substituted dithienyl DPP derivatives⁴⁶ possessed π - π stacking separated by a distance of 3.614 and 3.785 Å, respectively. In contrast, the insoluble basic phenyl H-bonded DPP derivative as reported by Głowacki *et al.*¹⁰ showed a 3.80 Å intermolecular π - π stacking distance. Thus, despite the fact that 'bulky' side groups like adamantyl tend to 'soften' the crystal and result in larger intermolecular distances, here it was observed that ethyladamantyl side groups result in a better intermolecular stacking between the conjugated cores. In general, compound (C) crystallizes in the monoclinic space group of *P21/c*, whereas 2-ethylhexyl *N*-substituted materials belong to the triclinic space group *P1* with *Z* = 4. Comparing the torsion angle of the thienyl group, it should be noted that one of the materials (C) was found to be of 1.79°, which is the smallest value in comparison with those previously reported for hexyl and ethyladamantyl *N*-substituted dithienyl DPP derivatives (6.37° and 6.64° respectively⁴⁶).

This phenomenon, inducing unusually short distances between conjugated DPP cores can be related to the specific structural properties of the adamantane molecule itself: bonded to the DPP(Th)₂ molecules, adamantyl groups create a distinctive 'triad' (Fig. 5) forming so-called herringbone aggregation. Thus, the ability of adamantyl groups to self-organize arranges the molecules in the crystal in plane-to-plane aggregation resulting in smaller π - π stacking distances between the conjugated cores. As far as the π - π interaction is a dominant charge-hopping

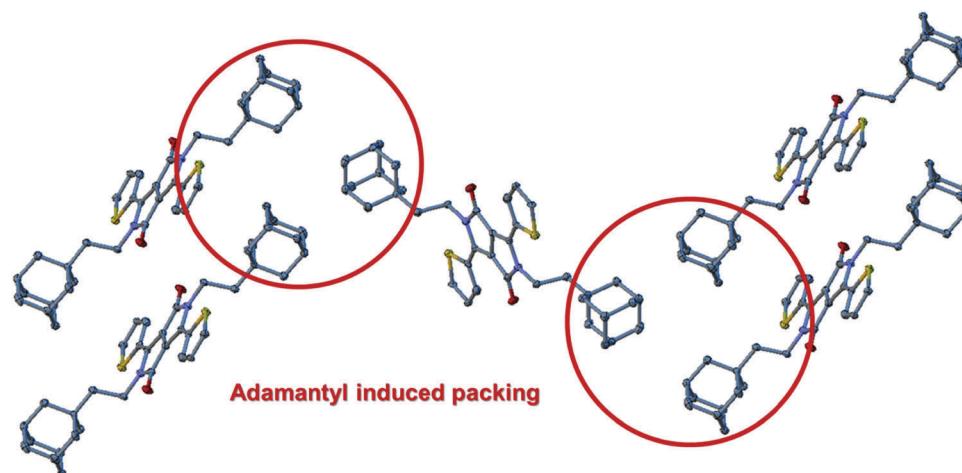


Fig. 5 Adamantyl-induced packing (in red circles) of the ethyladamantyl-substituted DPP derivative (XRD measurements).

pathway for DPPs,^{10,43} this material was proposed to be potentially attractive for electronic applications.

3.3. Field-effect mobilities

To investigate the field-effect mobilities, we fabricated OFETs with the three above-mentioned DPP derivatives in the bottom-gate/top-contact configuration. As can be seen from the transfer curves in Fig. 6, materials (A) and (B) showed hole-transport mobilities comparable with previously reported values for insoluble¹⁰ and soluble^{45,47} ($\mu_h \sim 10^{-3}$) derivatives. It should be noted that soluble DPP with 2-ethylhexyl side groups possessed slightly higher hole mobilities, which is in agreement with the

previously reported results,⁴³ where it was shown that the contribution of charge transport in the hydrogen-bonding direction is negligible, while transport mainly occurs along π -stacks or herringbone arrangements. Despite a previously reported theoretical prediction,⁴⁸ neither of the two above-mentioned materials were ambipolar, however, it was predicted that even though electron transport is advantageous in thiophene-substituted DPP, it is more sensitive to co-planarity (DPP-thienyl rotation angle) of the conjugated system. Indeed, looking at the absorption and emission spectra, one can notice that materials (A) and (B) have large Stokes shifts when the ethyladamantyl-substituted material clearly shows absorption and emitting maxima at zero-phonon transition with a negligible shift. In addition, intermolecular distances between DPP cores and thienyl rotational angles are lower in the ethyladamantyl-substituted derivative. A lower DPP-thienyl rotation angle can be the main reason why the material (C) showed an ambipolar behaviour, with an advantage of electron transport (Fig. 6C), as was predicted for dithienyl-substituted DPP.⁴⁸ It should be emphasized that hole-transport mobility values of the ethyladamantyl-substituted derivative exceeded by an order of magnitude those of both insoluble and soluble 2-ethylhexyl-substituted DPPs. Moreover, as was mentioned, more favourable electron-transport mobilities have reached a value of $0.2 \text{ cm}^2 \text{ V}^{-1} \text{ s}^{-1}$, which is comparable with the highest values for small-molecule DPP derivatives.³ However, previously reported results in most of the cases deal with electrophilic terminated substitution on the aromatic heterocycles,^{49–51} which resulted in higher conjugation, and thus π - π stacking, when in the present case an unsubstituted n-type DPP derivative is reported and ambipolar behaviour clearly related to crystalline organization, as far as *N*-substitution with ethyladamantyl groups does not significantly affect the position of the molecular orbitals in comparison with 2-ethylhexyl *N*-substitutions (Table 1).

Regarding the solution-processing technique, the above-described procedure does not allow the use of a TTC layer, as far as it is soluble in organic solvents. A composite low-surface-energy dielectric – TTC in the present case – secures a high level of molecular organization on the surface. Nevertheless, comparison of materials (B) and (C) has shown the advantage in the hole-transporting properties of the ethyladamantyl *N*-substituted sample over the 2-ethylhexyl substituted sample ($1.4 \times 10^{-7} \text{ cm}^2 \text{ V}^{-1} \text{ s}^{-1}$, $1 \times 10^{-8} \text{ cm}^2 \text{ V}^{-1} \text{ s}^{-1}$, respectively). Interestingly, no ambipolar behaviour was observed for material (C). On the one hand, this can be associated with the absence of a TTC

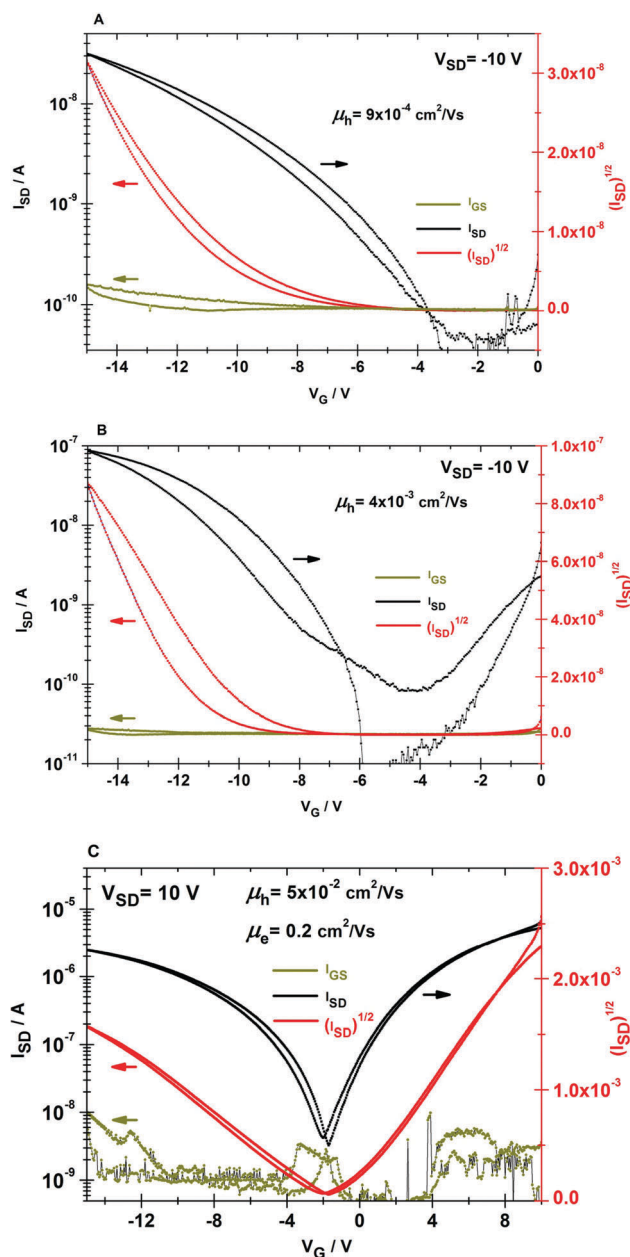


Fig. 6 Transfer curves of DPP-based OFET with gold source–drain electrodes (A) hydrogen, (B) 2-ethylhexyl and (C) ethyladamantyl *N*-substituted DPP(Th)₂.

Table 1 Energy orbitals (calculated), thiophene rotation dihedral angles and charge carrier mobilities

Material	HOMO (eV)	LUMO (eV)	α (°)	μ_e ($\text{cm}^2 \text{ V}^{-1} \text{ s}^{-1}$)	μ_h ($\text{cm}^2 \text{ V}^{-1} \text{ s}^{-1}$)
A	2.83	5.35	—	—	9×10^{-4}
B	2.69	5.16	6.64	—	4×10^{-3}
C	2.68	5.14	1.79	0.2	5×10^{-2}

Where: HOMO – highest occupied molecular orbital, LUMO – lowest unoccupied molecular orbital (B3LYP(6-311G*)^{52,53} calculated), α – single crystal XRD confirmed a thiophene rotation dihedral angle, μ_e and μ_h measured OFET charge carrier mobilities.

layer, thus it can result in low co-planarity of π - π conjugated cores on the surface; however, observation of low n-type mobility is generally the consequence of extrinsic effects or instability of radical anions to water, hydroxyl groups or oxygen.⁵⁴ In the present case, however, the gate surface was passivated with OTS; the large number of hydroxyl groups on the SiO₂ surface can act as traps for electrons injected into the organic semiconductor channel.^{55,56}

4. Conclusion

In conclusion, it can be summarized that DPP(Th)₂ derivatives containing adamantyl-derived solubilization side groups possessed hole mobilities of $5 \times 10^{-2} \text{ cm}^2 \text{ V}^{-1} \text{ s}^{-1}$, which are notably higher than the p-type mobilities of H- and 2-ethylhexyl-substituted derivatives ($9 \times 10^{-4} \text{ cm}^2 \text{ V}^{-1} \text{ s}^{-1}$ and $4 \times 10^{-3} \text{ cm}^2 \text{ V}^{-1} \text{ s}^{-1}$, respectively). Interestingly, as distinct from all the derivatives under investigation, the material with adamantyl-containing side groups showed an ambipolar behaviour. This is assumed to be due to the high crystallinity and co-planarity in the solid state. Evaluation of the thienyl group rotational angle with respect to the DPP core has shown that in comparison with the previously reported 2-ethylhexyl-substituted DPP(Th)₂ material, ethyladamantyl groups result in higher co-planarity of the conjugated cores. This correlates with a previously reported theoretical prediction where it was reported that electron transfer in dithienyl DPP is advantageous, however, sensitive to co-planarity (*i.e.* thienyl-DPP rotation angle).

In general, the above-described approach is very simple as it contains only one synthetic step, which is an important remark as far as both unsubstituted DPP and adamantane are commercially affordable common mass-produced materials. Moreover, the obtained mobility values were reached using a Au electrode, which is a significant advantage when the air-stability issue is considered. It also should be emphasized that this approach can be applied to a large portfolio of organic dyes, which are potentially attractive for organic electronics applications. Reaching a high solubility while preserving or improving high charge-carrier mobilities and thermal stability opens a path to a wide range of low-cost solution-processing techniques, such as coating and printing, as well as the ease of purification for the above-mentioned materials.

Acknowledgements

This work was supported by the Czech Science Foundation, Czech Republic *via* Project No. 13-29358S; research infrastructure was supported by Project MŠMT, Czech Republic No. LO1211. The MŠMT is also acknowledged for international cooperation project 7AMB15AT030. We gratefully acknowledge the financial support of Austrian Science Funds FWF within the Wittgenstein Prize for N. S. Sariciftci. Access to computing and storage facilities owned by parties and projects contributing to the National Grid Infrastructure MetaCentrum is appreciated. L. Fekete acknowledges financial support MŠMT LO1409 and SAFMAT LM2015088. We also acknowledge the CF X-ray diffraction and Bio-SAXS supported by the CIISB research infrastructure (LM2015043 funded by

MŠMT CR) for their support with obtaining scientific data presented in this paper.

References

- 1 Y. Li, P. Sonar, L. Murphy and W. Hong, *Energy Environ. Sci.*, 2013, **6**, 1684–1710, DOI: 10.1039/C3EE00015.
- 2 C. Kanimozhi, N. Yaacobi-Gross, E. K. Burnett, A. L. Briseno, T. D. Anthopoulos, U. Salzner and S. Patil, *Phys. Chem. Chem. Phys.*, 2014, **16**(32), 17253–17265, DOI: 10.1039/c4cp02322f.
- 3 W. S. Yoon, S. K. Park, I. Cho, J.-A. Oh, J. H. Kim and S. Y. Park, *Adv. Funct. Mater.*, 2013, **23**, 3519–3524, DOI: 10.1002/adfm.201203065.
- 4 T. Mukhopadhyay, B. Puttaraju, S. P. Senanayak, A. Sadhanala, R. Friend, H. A. Faber, T. D. Anthopoulos, U. Salzner, A. Meyer and S. Patil, *ACS Appl. Mater. Interfaces*, 2016, **8**(38), 25415–25427, DOI: 10.1021/acsami.6b08453.
- 5 S. Luňk Jr, M. Vala, J. Vyňuchala, I. Ouzzane, P. Horáková, P. Možíšková, Z. Eliáš and M. Weiter, *Dyes Pigm.*, 2011, **91**(3), 269–278, DOI: 10.1016/j.dyepig.2011.05.004.
- 6 M. Vala, J. Vyňuchal, P. Toman, M. Weiter and S. Luňk Jr., *Dyes Pigm.*, 2010, **84**(2), 176–182, DOI: 10.1016/j.dyepig.2009.07.014.
- 7 L. Fang, Y. Zhou, Y.-X. Yao, Y. Diao, W.-Y. Lee, A. L. Appleton, R. Allen, J. Reinspach, S. C. B. Mannsfeld and Z. Bao, *Chem. Mater.*, 2013, **25**(24), 4874–4880, DOI: 10.1021/cm4024259.
- 8 M. Sytnyk, E. D. Głowacki, S. Yakunin, G. Voss, W. Schöfberger, D. Kriegner, J. Stangl, R. Trotta, C. Gollner, S. Tollabimazraehno, G. Romanazzi, Z. Bozkurt, M. Havlicek, N. S. Sariciftci and W. Heiss, *J. Am. Chem. Soc.*, 2014, **136**, 16522–16532, DOI: 10.1021/ja5073965.
- 9 G. Chen, H. Sasabe, Y. Sasaki, H. Katagiri, X.-F. Wang, T. Sano, Z. Hong, Y. Yang and J. Kido, *Chem. Mater.*, 2014, **26**(3), 1356–1364, DOI: 10.1021/cm4034929.
- 10 E. D. Głowacki, H. Coskun, M. A. Blood-Forsythe, U. Monkowius, L. Leonat, M. Grzybowski, D. Gryko, M. Schuette White, A. Aspuru-Guzik and N. S. Sariciftcia, *Org. Electron.*, 2014, **15**(12), 3521–3528, DOI: 10.1016/j.orgel.2014.09.038.
- 11 E. D. Głowacki, M. Irimia-Vladu, M. Kaltenbrunner, J. Gsiorowski, M. S. White, U. Monkowius, G. Romanazzi, G. P. Suranna, P. Mastrorilli, T. Sekitani, S. Bauer, T. Someya, L. Torsi and N. S. Sariciftci, *Adv. Mater.*, 2013, **25**, 1563–1569, DOI: 10.1002/adma.201204039.
- 12 J. David, M. Weiter, M. Vala, J. Vyňuchal and J. Kučerka, *Dyes Pigm.*, 2011, **89**(2), 137–143, DOI: 10.1016/j.dyepig.2010.10.001.
- 13 E. D. Głowacki, L. Leonat, G. Voss, M.-A. Bodea, Z. Bozkurt, A. M. Ramil, M. Irimia-Vladu, S. Bauer and N. Serdar Sariciftci, *AIP Adv.*, 2011, **1**, 042132, DOI: 10.1063/1.3660358.
- 14 E. D. Głowacki, G. Voss, L. Leonat, M. Irimia-Vladu, S. Bauer and N. S. Sariciftci, *Isr. J. Chem.*, 2012, **52**, 1–12, DOI: 10.1002/ijch.201100130.
- 15 E. Coatanéa, V. Kantola, J. Kulovesi, R. Lahti, R. Lin and M. Zavodchikova, in *Printed Electronics, Now and Future*,

- ed. Y. Neuvo and S. Ylönen, 2009, pp. 63–102, ISBN 978-952-248-078-1.
- 16 K. A. Mazzio and C. K. Luscombe, *Chem. Soc. Rev.*, 2015, **44**, 78–90, DOI: 10.1039/C4CS00227J.
 - 17 W. Cao and J. Xue, *Energy Environ. Sci.*, 2014, **7**, 2123–2144, DOI: 10.1039/C4EE00260A.
 - 18 A. Guerrero and G. Garcia-Belmonte, *Nano-Micro Lett.*, 2016, **9**(1), 10, DOI: 10.1007/s40820-016-0107-3.
 - 19 S. Muench, A. Wild, C. Friebe, B. Häupler, T. Janoschka and U. S. Schubert, *Chem. Rev.*, 2016, **116**(16), 9438–9484, DOI: 10.1021/acs.chemrev.6b00070.
 - 20 N. Thejo Kalyani and S. J. Dhole, *Renewable Sustainable Energy Rev.*, 2012, **16**, 2696–2723, DOI: 10.1016/j.rser.2012.02.021.
 - 21 M. Vala, M. Weiter, J. Vyňuchal, P. Toman and S. Luňák Jr., *J. Fluoresc.*, 2008, **18**, 1181–1186, DOI: 10.1007/s10895-008-0370-x.
 - 22 J. B. Kim, C. Fuentes-Hernandez, D. K. Hwang, S. P. Tiwari, W. J. Potscavage Jr. and B. Kippelen, *Org. Electron.*, 2011, **12**(7), 1132–1136, DOI: 10.1016/j.orgel.2011.04.007.
 - 23 M. Jakesova, D. H. Apaydin, M. Sytnyk, K. Oppelt, W. Heiss, N. S. Sariciftci and E. D. Głowacki, *Adv. Funct. Mater.*, 2016, **26**, 5248–5254, DOI: 10.1002/adfm.201601946.
 - 24 C. Yumusak, M. Abbas and N. S. Sariciftci, *J. Lumin.*, 2013, **134**(1–2), 107–112, DOI: 10.1016/j.jlumin.2012.09.003.
 - 25 E. D. Głowacki, G. Romanazzi, C. Yumusak, H. Coskun, U. Monkowius, G. Voss, M. Burian, R. T. Lechner, N. Demitri, G. J. Redhammer, N. Sünger, G. P. Suranna and S. Sariciftci, *Adv. Funct. Mater.*, 2015, **25**, 776–787, DOI: 10.1002/adfm.201402539.
 - 26 N. Martino, D. Ghezzi, F. Benfenati, G. Lanzani and M. R. Antognazza, *J. Mater. Chem. B*, 2013, **1**, 3768–3780, DOI: 10.1039/C3TB20213E.
 - 27 A. N. Sokolov, M. E. Roberts and Z. Bao, *Mater. Today*, 2009, **12**(9), 12–20, DOI: 10.1016/S1369-7021(09)70247-0.
 - 28 R. C. Fort and P. v. R. Schleyer, *Chem. Rev.*, 1964, **64**(3), 277–300, DOI: 10.1021/cr60229a004.
 - 29 J. Krajčovič, A. Kovalenko, P. Heinrichová, M. Vala and M. Weiter, *J. Lumin.*, 2016, **175**, 94–99, DOI: 10.1016/j.jlumin.2016.02.019.
 - 30 M. M. Lohrengel, *Mater. Sci. Eng., R*, 1993, **11**, 243–294, DOI: 10.1016/0927-796X(93)90005-N.
 - 31 M. Kaltenbrunner, P. Stadler, R. Schwödiauer, A. W. Hassel, N. S. Sariciftci and S. Bauer, *Adv. Mater.*, 2011, **23**, 4892–4896, DOI: 10.1002/adma.201103189.
 - 32 M. Kraus, S. Richler, A. Opitz, W. Brütting, S. Haas, T. Hasegawa, A. Hinderhofer and F. Schreiber, *J. Appl. Phys.*, 2010, **107**, 094503, DOI: 10.1063/1.3354086.
 - 33 A. Opitz, M. Horlet, M. Kiwull, J. Wagner, M. Kraus and W. Brütting, Bipolar charge transport in organic field-effect transistors: enabling high mobilities and transport of photo-generated charge carriers by a molecular passivation layer, *Org. Electron.*, 2012, **13**, 1614–1622, DOI: 10.1016/j.orgel.2012.04.032.
 - 34 Y. Wang and M. Lieberman, *Langmuir*, 2003, **19**(4), 1159–1167, DOI: 10.1021/la020697x.
 - 35 A. Kovalenko, J. Honová, M. Vala, S. Luňák, L. Fekete, P. Horáková, L. Dokládlová, L. Kubč and M. Weiter, *Int. J. Photoenergy*, 2015, 1–9, DOI: 10.1155/2015/734917.
 - 36 Z. Ding, J. Kettle, M. Horie, S. W. Chang, G. C. Smith, A. I. Shames and E. A. Katz, *J. Mater. Chem. A*, 2016, **4**, 7274–7280, DOI: 10.1039/C6TA00721J.
 - 37 A. E. Rudenko, P. P. Khlyabich and B. C. Thompson, *Polym. Chem.*, 2016, **54**, 1526–1536, DOI: 10.1002/pola.28007.
 - 38 M. Saito, I. Osaka, Y. Suzuki, K. Takimiya, T. Okabe, S. Ikeda and T. Asano, *Sci. Rep.*, 2015, **5**, 14202, DOI: 10.1038/srep14202.
 - 39 M. Li, F. Hinkel, K. Müllen and W. Pisula, *Nanoscale*, 2016, **8**, 9211–9216, DOI: 10.1039/C6NR01082B.
 - 40 C. Bathula, S. K. Lee, P. Kalode, S. Badgular, N. S. Belavagi, I. A. M. Khazi and Y. Kang, *J. Fluoresc.*, 2016, **26**(3), 1045–1052, DOI: 10.1007/s10895-016-1792-5.
 - 41 B. Calmettes, N. Estrampes, C. Coudret, T. J. Roussel, J. Farauto and R. Coratger, *Phys. Chem. Chem. Phys.*, 2016, **18**, 20281, DOI: 10.1039/c5cp06733b.
 - 42 F. Würthner, T. E. Kaiser and C. R. Saha-Möller, *Angew. Chem., Int. Ed.*, 2011, **50**, 3376–3410, DOI: 10.1002/anie.201002307.
 - 43 J. Dhar, D. P. Karothu and S. Patil, *Chem. Commun.*, 2015, **51**, 97, DOI: 10.1039/c4cc06063f.
 - 44 S. Luňák Jr, M. Vala, J. Vyňuchal, I. Ouzzane, P. Horáková, P. Možíšková, Z. Eliáš and M. Weiter, *Dyes Pigm.*, 2011, **91**(3), 269–278, DOI: 10.1016/j.dyepig.2011.05.004.
 - 45 A. K. Palai, H. Cho, S. Cho, T. J. Shin, S. Jang, S.-U. Park and S. Pyo, *Org. Electron.*, 2013, **14**, 1396–1406, DOI: 10.1016/j.orgel.2013.03.002.
 - 46 M. A. Naik, N. Venkatramaiah, C. Kanimozhi and S. Patil, *J. Phys. Chem. C*, 2012, **116**, 26128–26137, DOI: 10.1021/jp306365q.
 - 47 J. Kwon, H. Na, A. K. Palai, A. Kumar, U. Jeong, S. Cho and S. Pyo, *Synth. Met.*, 2015, **209**, 240–246, DOI: 10.1016/j.synthmet.2015.07.015.
 - 48 J. Calvo-Castro, C. J. McHugh and A. J. McLean, *Dyes Pigm.*, 2015, **113**, 609–617, DOI: 10.1016/j.dyepig.2014.09.031.
 - 49 Y. Qiao, Y. Guo, C. Yu, F. Zhang, W. Xu, Y. Liu and D. Zhu, *J. Am. Chem. Soc.*, 2012, **134**, 4084–4087, DOI: 10.1021/ja3003183.
 - 50 X. Liu, L. Chen, L. Hu and Y. Chen, *J. Phys. Chem. C*, 2015, **119**(46), 25887–25897, DOI: 10.1021/acs.jpcc.5b07349.
 - 51 Y. Li, P. Sonar, L. Murphy and W. Hong, *Energy Environ. Sci.*, 2013, **6**, 1684–1710, DOI: 10.1039/C3EE00015J.
 - 52 M. J. Frisch, G. W. Trucks, H. B. Schlegel, G. E. Scuseria, M. A. Robb, J. R. Cheeseman, G. Scalmani, V. Barone, B. Mennucci, G. A. Petersson, H. Nakatsuji, M. Caricato, X. Li, H. P. Hratchian, A. F. Izmaylov, J. Bloino, G. Zheng, J. L. Sonnenberg, M. Hada, M. Ehara, K. Toyota, R. Fukuda, J. Hasegawa, M. Ishida, T. Nakajima, Y. Honda, O. Kitao, H. Nakai, T. Vreven, J. A. Montgomery, Jr., J. E. Peralta, F. Ogliaro, M. Bearpark, J. J. Heyd, E. Brothers, K. N. Kudin, V. N. Staroverov, R. Kobayashi, J. Normand, K. Raghavachari, A. Rendell, J. C. Burant, S. S. Iyengar, J. Tomasi, M. Cossi, N. Rega, J. M. Millam, M. Klene, J. E. Knox, J. B. Cross,

- V. Bakken, C. Adamo, J. Jaramillo, R. Gomperts, R. E. Stratmann, O. Yazyev, A. J. Austin, R. Cammi, C. Pomelli, J. W. Ochterski, R. L. Martin, K. Morokuma, V. G. Zakrzewski, G. A. Voth, P. Salvador, J. J. Dannenberg, S. Dapprich, A. D. Daniels, Ö. Farkas, J. B. Foresman, J. V. Ortiz, J. Cioslowski and D. J. Fox, *Gaussian 09, Revision E.01*, Gaussian, Inc., Wallingford CT, 2009.
- 53 A. D. Becke, *J. Chem. Phys.*, 1993, **98**, 5648–5652, DOI: 10.1063/1.464913.
- 54 V. Kažukauskas, H. Tzeng and S. A. Chen, *Appl. Phys. Lett.*, 2002, **80**, 2017, DOI: 10.1063/1.1459114.
- 55 E. C. P. Smits, T. D. Anthopoulos, S. Setayesh, E. van Veenendaal, R. Coehoorn, P. W. M. Blom, B. de Boer and D. M. de Leeuw, *Phys. Rev. B: Condens. Matter Mater. Phys.*, 2006, **73**, 205316, DOI: 10.1103/PhysRevB.73.205316.
- 56 L. L. Chua, J. Zaumseil, J. F. Chang, E. C. W. Ou, P. K. H. Ho, H. Sirringhaus and R. H. Friend, *Nature*, 2005, **434**, 194, DOI: 10.1038/nature03376.